Numerical prediction of nonlinear rheology of branched polymer melts

Chinmay Das, Daniel J. Read, Dietmar Auhl, Michael Kapnistos, Jaap den Doelder, Iakovos Vittorias, and Tom C. B. McLeish

Citation: Journal of Rheology **58**, 737 (2014); doi: 10.1122/1.4869485
View online: http://dx.doi.org/10.1122/1.4869485
View Table of Contents: http://scitation.aip.org/content/sor/journal/jor2/58/3?ver=pdfcov
Published by the The Society of Rheology

Numerical prediction of nonlinear rheology of branched polymer melts

Chinmay Das[a)]

School of Physics and Astronomy, University of Leeds, Leeds LS2 9JT, United Kingdom

Daniel J. Read[b)]

Department of Applied Mathematics, University of Leeds, Leeds LS2 9JT, United Kingdom

Dietmar Auhl[c)]

Faculty of Humanities and Sciences, Maastricht University, P. O. Box 616, 6200 MD Maastricht, The Netherlands

Michael Kapnistos[d)]

Plastika Kritis S.A., P. O. Box 1093, GR 711 10 Iraklion, Crete, Greece

Jaap den Doelder[e)]

Dow Benelux B.V., Performance Plastics Materials Science, P. O. Box 48, 4530 AA Terneuzen, The Netherlands

Iakovos Vittorias[f)]

Bassel Polyolefine GmbH, LyondellBasell, R&D Polymer Physics and Characterization, Industriepark Hoechst, D-65926 Frankfurt am Main, Germany

Tom C. B. McLeish[g)]

Departments of Physics and Chemistry, Durham University, Durham DH1 3LE, United Kingdom

(Received 10 October 2013; final revision received 13 March 2014; published 1 April 2014)

[a)]Author to whom correspondence should be addressed; electronic mail: c.das@leeds.ac.uk
[b)]Electronic mail: d.j.read@leeds.ac.uk
[c)]Electronic mail: dietmar.auhl@maastrichtuniversity.nl
[d)]Electronic mail: m.kapnistos@gmail.com
[e)]Electronic mail: cfdendoelder@dow.com
[f)]Electronic mail: iakovos.vittorias@lyondellbasell.com
[g)]Electronic mail: t.c.b.mcleish@durham.ac.uk

Synopsis

In a recent short communication [Read, D. J. *et al.*, Science **333**, 1871 (2011)], we showed that a computational scheme can describe the nonlinear flow properties for a series of industrial low-density polyethylene (LDPE) resins starting from the molecular architecture. The molecular architecture itself is determined by fitting parameters of a reaction kinetics model to average structural information obtained from gel-permeation chromatography and light scattering. Flow responses of these molecules in transient uniaxial extension and shear are calculated by mapping the stretch and orientation dynamics of the segments within the molecules to effective pom-pom modes. In this paper, we provide the details of the computational scheme and present additional results on a LDPE and a high-density polyethylene resin to illustrate the dependence of segmental maximum stretch variables on the flow rate. © *2014 The Society of Rheology*. [http://dx.doi.org/10.1122/1.4869485]

I. INTRODUCTION

Predicting the flow properties of entangled branched polymer melts from their molecular structure remains one of the hard problems of polymer physics. It also attracts, understandably, considerable industrial interest. The very large separation of the relevant relaxation timescales renders traditional molecular simulations like molecular dynamics or Monte Carlo of little use for industrial polymer resins. Similarly, extensions of liquid state theories to predict the flow properties have had limited success. However, in the last decade, considerable success has been found in the case of linear rheology by using the phenomenological relaxation mechanisms of extended tube theory [Doi and Edwards (1986); de Gennes (1971)] to follow numerically the relaxation of a set of representative molecules defined at the segment level [Larson (2001); Park *et al.* (2005); Das *et al.* (2006a)]. These "hierarchical" relaxation algorithms work by using a faithful representation of the reaction chemistry to generate an *ensemble of molecules in-silico*. To probe at the experimentally relevant timescale, a description of the molecules at the level of entanglement segments suffices. After a small step strain, coupled phenomenological rules give the time relaxation of stress carrying segments at discrete times. The viscoelastic moduli are then calculated by assigning the weights calculated during the previous step to the set of Maxwell modes defined at those quasicontinuous times. This approach has met with considerable success for a wide variety of both model and industrial resins, despite requiring only two chief fitting parameters for each polymer chemistry (the chemistry-dependent entanglement molar mass M_e and the entanglement time τ_e). In addition, two more chemistry-independent, dimensionless, order-one parameters, related to the dynamic tube dilation through constraint release and the branch-point hop size, are required.

In this paper, we describe an extension of such a computational scheme for predicting the nonlinear flow properties of generic branched polymer melt. The linear rheology is calculated from a set of Maxwell modes, with the weights and relaxation times of the Maxwell modes computed from following the relaxation of the representative molecules in time. Correspondingly, we calculate the nonlinear rheological response from a set of pom-pom modes [McLeish and Larson (1998)], with the appropriate parameters of these pom-pom modes computed from the relaxation after a small step strain. We highlight here the four nontrivial aspects of this work at the very outset: First, multimode pom-pom equations [Inkson *et al.* (1999)] frequently have been used to fit the nonlinear rheological response of branched polymers, but we are aiming for *a priori* prediction and not a fit of experimental data in this work. Thus, the priority variables and the relaxation times appearing in the pom-pom equations are endowed with a physical meaning from the

topological structure and stress relaxation timescales. Second, to predict the linear rheology correctly, one uses two sets of Maxwell modes—one for the stress relaxed by the chains and another for the stress carried by the tube constraints themselves. We extend the use of pom-pom modes in a manner that is consistent with this constraint release picture. Third, the geometric concept of *priority variable* [Bick and McLeish (1996)] has been used in the literature to assign the maximum stretch of segments in a branched molecule. But, as we show in this work, one needs to modify the "bare" geometric priority so that it becomes flow rate dependent. Finally, it is nontrivial that the topological connectivity of the molecules and the computation required to predict the linear rheological response alone contain enough information for accurate prediction of the stress growth and relaxation in the nonlinear regime. Since we know that the pom-pom equations are versatile enough to fit both the extensional and shear results found in experiments of complex-architecture melts [McLeish and Larson (1998); Inkson *et al.* (1999); Lee *et al.* (2001)], if we find a way to assign proper weights to possibly a large number of such modes, the hope is that we can capture the nonlinear rheology properly. But, the ultimate success of the scheme rests through comparison with experimental results. By comparing our predictions with the experimental data on the stress profile during startup uniaxial extension and shear flow for some industrial resins, we show that the scheme is fairly successful, given there are no extra free parameters beyond those already present for predicting the linear rheology.

The rest of the paper is organized as follows: We begin with a short recapitulation of the scheme used for predicting the linear rheology of generic branch-on-branch polymer melt [Das *et al.* (2006a)] in Sec. II. Next, we give a brief summary of the pom-pom constitutive equations and previous attempts in assigning pom-pom parameters to branched polymer resins (Sec. III). These two introductory sections are brief and serve only to introduce the variables used in rest of the paper. The new physics included in marrying the pom-pom equations with the hierarchical relaxation scheme is in Sec. IV. Section V gives a detailed description of the algorithm. The scheme is included in the publicly available software to calculate rheological properties [Das (2012)]. We consider an industrial branched low-density polyethylene (LDPE) resin and a metallocene catalyzed high-density polyethylene (HDPE) resin to test the predictive power of the algorithm in Sec. VI.

A short description of the algorithm and results on a series of LDPE resins have been published elsewhere [Read *et al.* (2011)]. The description of the algorithm in that work was necessarily too short to provide all the important details for a critical evaluation of the scheme, or for others to build on this work. We end this paper with a summary including our own views of shortcomings in the scheme and an outlook on the possible extensions to this work.

II. COMPUTATIONAL LINEAR RHEOLOGY

The generalization of the process of arm-retraction from simple entangled star polymers [Milner and McLeish (1997)] to more complex branched architecture was initially investigated analytically in a few simple cases [McLeish (1988); Rubinstein *et al.* (1990)]. The coupled nature of the relaxation prohibits an analytical description without drastic simplifications for industrially relevant resins with large topological polydispersity. Larson (2001) introduced the hierarchical numerical relaxation scheme based on the tube model of de Gennes (1971) and Doi and Edwards (1986) for branched polymer melts. Das *et al.* (2006a) extended the scheme for generic branch-on-branch polymers.

For distinguishing between the two, we use the already common terminology of "hierarchical model" for Larson (2001) and extensions by Larson and collaborators and "BoB" for Das *et al.* (2006a). For molecules which can be cast as a comb or star polymer, both models follow very similar physics and differ only in details. A comparative analysis of the two has been recently done by Wang *et al.* (2010). We should also note here a rather different approach for numerical prediction of linear rheology by van Ruymbeke *et al.* (2006). Of these, only the BoB code is generic enough to handle the highly branched structure that arises in polymers like LDPE.

A number of articles already cover the methodology used in calculating the rheological response of branched polymers in the linear regime in BoB [Das *et al.* (2006a); Das *et al.* (2006b); Wang *et al.* (2010)]. We only summarize the main ideas here, chiefly to introduce the variables that are required in the calculation of the nonlinear rheology.

Figure 1 summarizes the relaxation schemes considered in computational linear rheology. In the dense environment of melt, the topological constraint of noncrossing gives rise to the effective confinement of a given strand of a molecule in a tube potential due to all the other molecules. The tube diameter a sets the length scale for the problem. The entanglement molar mass M_e, the molar mass of a chain having the same size as the tube diameter, is used to express the length Z of the polymer segments. The entanglement time τ_e, the Rouse relaxation time for a linear polymer of length equal to the tube diameter, is used as the unit of time.

After a small step strain, at early times, only the chain ends can explore new conformations through withdrawal in the tube and subsequent sampling of uncorrelated tube constraints. In this process, the stress carried by the part of the old tube, that is renewed, is lost. The variable $z(t)$ defines the length of the tube, measured from the free end, that has relaxed. Once a *side arm* retracts its whole length (at time τ_a), it assigns an extra drag ζ_a on the *backbone*, localized at the branch point, given by

$$\zeta_a = \frac{2k_B T \tau_a}{p^2 a(\tau_a)^2}, \tag{1}$$

where k_B is the Boltzmann constant and T is the temperature. The parameter p fixes the diffusive hop length scale and $a(\tau_a)$ is the tube diameter relevant at τ_a. Strands with one or more localized drag-points from side arm collapse are termed *compound arms*. The arm-retraction mechanism becomes more subtle when branch points on compound arms, deeper than the currently relaxing tube segments, become mobilized themselves. The subsequent fluctuations of such branch points can contribute to the relaxation of the free ends. A good approximation to this retraction of compound arms considers an effective segment length $\tilde{Z}$, which itself has a Rouse-like dynamics with friction centers coming from the relaxed side arms [Das *et al.* (2006a)]. $\tilde{Z}(t)$ gives the pivot point about which the compound arm undergoes coherent fluctuations at time t. Equivalently, the time t at which $\tilde{Z}$ reaches a certain part of a molecule assigns an approximate Rouse time for that part. Once the leftover backbone becomes effectively linear, it can relax by reptation—a faster mechanism compared to deep arm-retraction.

Since the tube constraint is due to all the other molecules, which themselves are relaxing at the same time, the tube constraint is itself time dependent. Phenomenologically (with some scaling level theoretical backing [Colby and Rubinstein (1990)], this is described by tube dilation—where the tube diameter scales with ϕ, the amount of unrelaxed material $(a(t) = a\phi^{-\alpha})$. Thus, with relaxation, the tube diameter increases (the confining potential softens), which in turn increases the rate of relaxation. The coupling

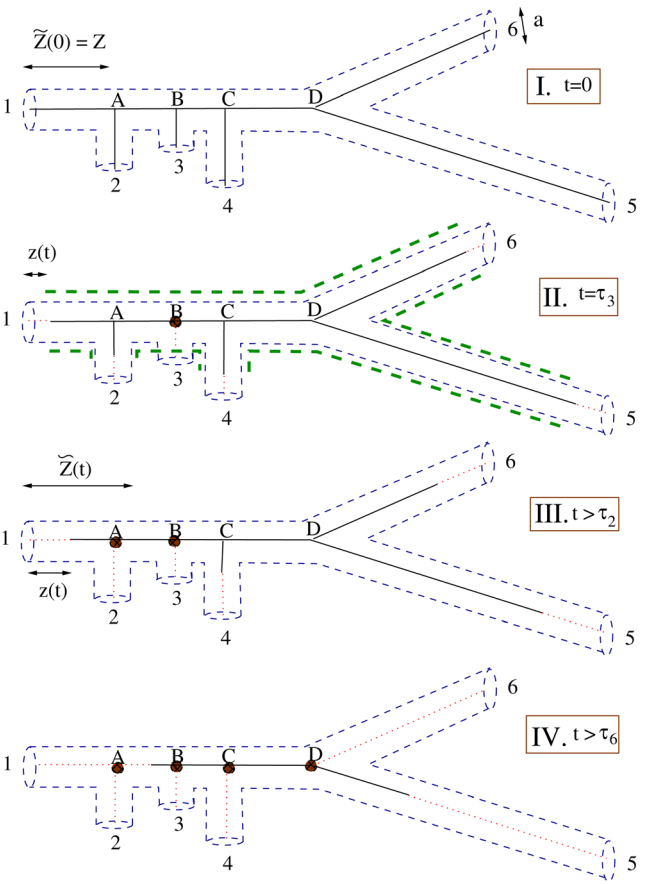

FIG. 1. Schematic representation of hierarchical stress relaxation: (I) Relaxation of stress carried by a given polymer (represented by solid line) after a small step strain is hindered by the tube potential (diameter a, drawn as dashed line). Free-ends (labeled by numbers) of length Z retract as star-arms. (II) For $t > \tau_3$ (the retraction time of segment 3), the branch point B provides localized friction (indicated by filled circle). The relaxation of material softens the confining potential, indicated by thick dashed lines around the original tube. $z(t)$ designates the length of the original tube segment lost at time t, measured from the end-monomer of a free-end. (III) Beyond τ_2, the relaxation time of segment 2, the free-end 1 can retract by any combination of the inner segments, hindered by the localized frictions from the relaxed side arms. This assigns a dynamics to $\tilde{Z}$, the pivot point of retraction, determined by the localized frictions at branch points. (IV) At long times (here, $t > \tau_6$), the unrelaxed segments behave like a linear molecule and can relax by reptation.

between the different molecules is expressed by determining the tube diameter in a self-consistent way. The current effective/dilated tube at relaxation time t is termed the "supertube." The entanglement density experienced by the segments due to the supertube is denoted by $\phi_{ST}(t)$. Except for those times in which some fraction of the molecules undergoes rapid relaxation, ϕ_{ST} follows ϕ.

Figure 1 illustrates the above relaxation mechanisms for a specific molecule. In particular, it shows (I) the initial unrelaxed topology of the molecule in tube co-ordinates; (II) relaxation of side arms, with corresponding tube dilution and softening of the potential; (III) full relaxation of side arms and mobilization of branch points, allowing deeper relaxation of a compound arm; (IV) terminal relaxation by reptation of a linearlike segment. A detailed commentary of these stages for the specific molecule is given in the figure caption.

The stress relaxation is calculated as

$$G(t) = G_0 \int_0^{\infty} e^{-t/\tau} \left[-\frac{d}{dt}\left(\phi(t)\phi_{ST}(t)^{\alpha}\right) \right]_{\tau} d\tau. \tag{2}$$

Here, G_0 is the plateau modulus [$G_0 \simeq (4/5)(cRT/M_e)$, with c being the polymer density and R the universal gas constant].

III. PRIORITY VARIABLE AND POM-POM CONSTITUTIVE EQUATIONS

Bick and McLeish (1996) introduced the concept of priority variable to describe the damping function for the nonlinear stress relaxation in polymers containing long-chain branching, where the experimental damping function for the relaxation modulus is found to be much weaker than that predicted by the Doi-Edwards damping function. A large strain increases the contour length between branch points, which are not (initially) free to retract along confining tubes in the same way as a free end. The consequent segmental stretch enhances the elastic stress. However, at higher strains, an imbalance in the tensions along segments connected to a branch point can cause "branch-point retraction" along the tube containing the most stretched segment. At short times, the force balance at the branch points gives a maximum tension needed before the branch point can retract. For a chain segment between branch points, priority was defined as the ratio of the maximum permissible tension to the equilibrium tension of that chain segment. The entropic nature of the tensions gives rise to a simple geometrical picture (Fig. 2). For any given strand, one counts the number of free ends on the left n_L and the same on the right n_R of that segment. The minimum of these two defines the priority of the segment. The priority is the value of the local chain stretch at the point of branch point withdrawal; the chain segment is assumed to maintain that maximum stretch at all higher strains.

For a general long chain branched polymer, the relaxation times vary widely (relaxation time depends exponentially on the "depth" of a segment in a molecule). Thus, the geometric criteria given above do not capture the maximum tension in a given segment at all flow rates. Read and McLeish (2001) introduced the idea of "snipped" priority. They identified a timescale associated with the flow (τ_{F}, the inverse of flow rate) and suggested that segments which relax faster than this timescale should be neglected in calculation of the priority. Thus, in Fig. 3, the segments having relaxation times shorter than τ_{F} are replaced by "blobs" signifying localized frictional drags, which do not contribute to the priority calculation. Effectively, the molecule in Fig. 3 behaves like an "H" polymer with a single backbone capable of supporting a (dimensionless) stretch of $\lambda = 2$. The snipped priority underestimates the extension hardening severely; this was clear in the original work of Read and McLeish (2001), even bearing in mind the approximations in their scheme. We confirm this observation more quantitatively below in Fig. 8. Nevertheless, the concept of a snipped priority gives useful insights toward building a model for flow-modified priority developed in this work.

A simpler class of polymers, pom-pom polymers comprising a single backbone with q identical side arms at the both ends, allow a simple constitutive equation that successfully captures the stress profile in nonlinear flow [Bisko *et al.* (1997); McLeish and Larson (1998)]. The number of side arms q gives the maximum permissible tension on the backbone and hence gives the priority of the backbone. The pom-pom equations are simple because all the side arms have the same timescales of retraction, and the stress contribution is assumed to be dominated by the backbone. The dynamics of the stretch relaxation

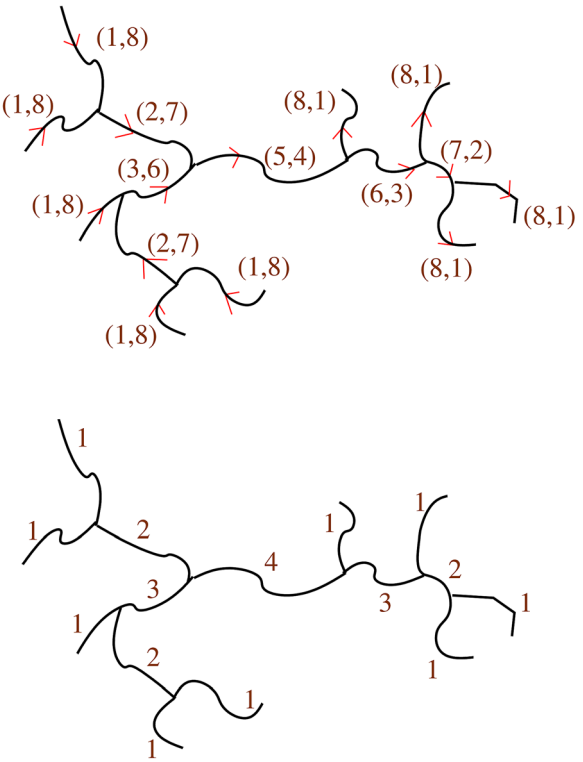

FIG. 2. Priority variables for a branched molecule. (a) For a given strand, we count n_L, the number of free ends on the left (against the arrow), and n_R on the right (along the arrow heads). (b) Geometric priorities are defined by the smaller of these two numbers.

of the backbone is governed by the balance of the entropic tension and the localized frictional force at the branch points. This gives an upper bound on the elastic force and hence on the stretch λ of the backbone. For faster flow, the branch points will withdraw in the backbone tube and no further increase of stretch is possible. McLeish and Larson (1998)

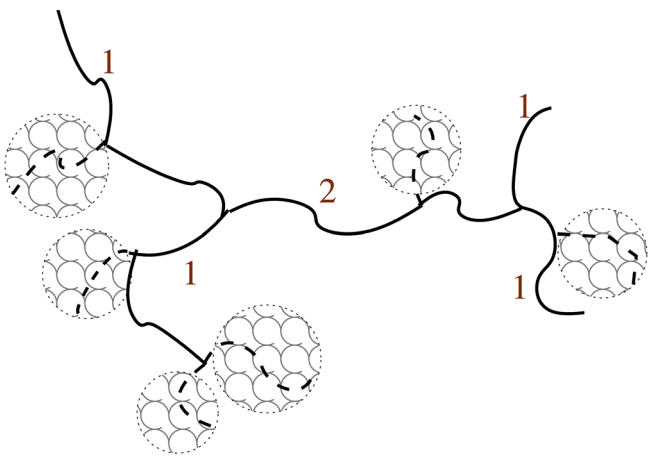

FIG. 3. Snipped priority [Read and McLeish (2001)] for the same molecule as in Fig. 2 at a certain flow rate. The segments having relaxation times shorter than the inverse flow rate are replaced by blobs signifying localized frictional drags.

also considered the coupled dynamics for the branch-point withdrawal. Later authors [Inkson *et al.* (1999); Blackwell *et al.* (2000)] neglected this dynamics of branch points because of the large separation of timescales for branch point withdrawal and stretch relaxation. For a numerical calculation, as in this work, the natural choice is the differential approximation of the constitutive equation connecting the stress $\boldsymbol{\sigma}$ with the orientational tensor $\mathbf{S}$

$$\boldsymbol{\sigma} = 3G\lambda^2(t)\mathbf{S}, \tag{3}$$

with $\mathbf{S} \equiv \mathbf{A}/\mathrm{tr}(\mathbf{A})$ determined through the auxiliary tensor $\mathbf{A}$ satisfying the upper convective Maxwell model

$$\frac{D}{Dt}\mathbf{A} = \mathbf{K}\cdot\mathbf{A} + \mathbf{A}\cdot\mathbf{K}^T - \frac{1}{\tau_o}(\mathbf{A}-\mathbf{I}). \tag{4}$$

Here, $D/Dt \equiv (\partial/\partial t) + \mathbf{v}.\nabla$ is the convective derivative, $\mathbf{K}$ is the deformation rate tensor, $\mathbf{I}$ is the identity tensor, and τ_o is the orientational relaxation time of the backbone. The dynamics of the stretch λ is given by

$$\frac{D}{Dt}\lambda = \lambda\mathbf{K}:\mathbf{S}^T - \frac{1}{\tau_s}(\lambda-1)\exp\left[\frac{2}{q-1}(\lambda-1)\right], \tag{5}$$

with τ_s being the stretch relaxation time of the backbone. For an ensemble of different pompom molecules, the stress is assumed to be additive. Thus, each of the pompom molecules is characterized by its weight fraction determining G in the stress contribution, number of side arms at each end q, the orientational relaxation time τ_o, and the stretch relaxation time τ_s. The lengths of the backbone and the dangling arms together determine the prefactor G in the stress equation in the original formulation.

IV. COMPUTATIONAL NONLINEAR RHEOLOGY

The simplicity of obtaining the numerical solution for nonlinear flow behavior of pom-pom model led to considerable work toward mapping an arbitrarily branched molecule to pom-pom modes. Multimode pom-poms have been used successfully to fit the nonlinear extensional and shear rheology data [Inkson *et al.* (1999)]. The distributions of the timescales and of the priorities for highly branched resins like LDPE do not strongly depend on the number of modes selected for data fitting, which suggests that the continuous limiting form of the fitting parameters as a function of mode relaxation time may have direct relationship to the polymers themselves. However, when one considers modeling of simple polymers, where the structure is known, the fitting parameters in general do not bear any resemblance to the geometric priority q or snipped priority q_S [Inkson *et al.* (1999)]. Thus, in spite of considerable success of fitting both extensional and shear startup, extension hardening, and shear thinning at a number of flow rates, such exercises so far lacked predictive power for a resin where the structure is known, but the rheological data are absent on which to fit the model parameters.

A. Pom-pom modes accounting for distribution in orientational relaxation times

The resolution in pom-pom modes must reproduce the linear envelope decided by the linear rheology. Coarse graining over a time interval Δt at t_M, Eq. (2), resolves the

stress relaxation to a set of Maxwell modes with the associated modulus g_M (t_M) given by

$$-\frac{g_M}{G_0} = \left[\phi_{ST}^{\alpha}\right]\Delta\phi + \left[\alpha\phi_{ST}^{\alpha-1}\phi\right]\Delta\phi_{ST}. \tag{6}$$

Here, $\Delta\phi$ is the change in the amount of unrelaxed fraction in the time interval Δt and $\Delta\phi_{ST}$ is the change in the entanglement density experienced at the same interval. We interpret the two terms on the right-hand side of Eq. (6) containing $\Delta\phi$ and $\Delta\phi_{ST}$, respectively, as describing the stress relaxation due to escape from the confining tube constraint and due to the constraint release on the remaining chains trapped in the tube potential at this timescale (Fig. 4). This prompts us to consider two separate sets of pom-pom modes: "Tube escape modes" and "constraint release modes." Both of these two sets of modes share the same orientational relaxation time $(\tau_o = \tau_M)$, but the priority and the stretch relaxation time distribution are determined by the currently relaxing parts of the chains for the tube escape modes and by the unrelaxed part of the chains for the constraint release modes.

B. Stretch time distribution

Stretch in a part of a molecule relaxes via motion in which chain tension acts against local friction: Either monomeric friction from the background melt or, in the case of a compound branched arm, much larger friction arising from side chain motion. For the outer most branches, we consider that chain tension balances monomeric friction only, so that $\tau_s = z^2\tau_e/4$ (obtained as the Rouse time of that arm, when pinned at one end). For inner segments, we require the effective "Rouse time" when friction is considered to arise from side arms. Fortunately, the relevant calculation is already embedded within the original BoB algorithm since, as outlined in Sec. II, the pivot point location $\tilde{Z}(t)$ is obtained

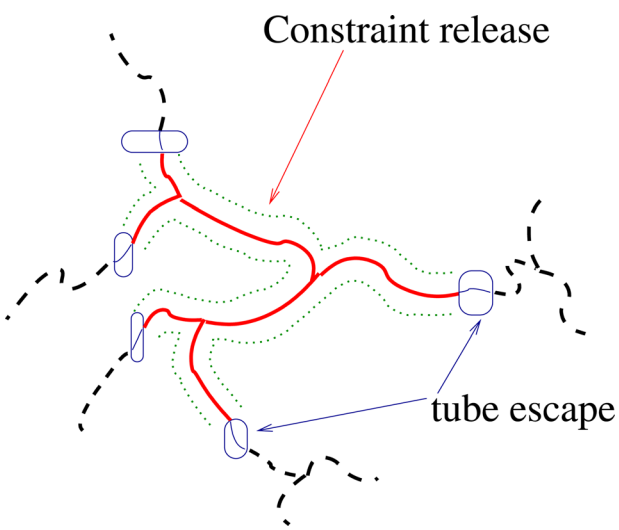

FIG. 4. Molecular contributions to stress decay: The boxed thin lines represent parts of the molecule having relaxation time τ_M and contributes as "tube escape pom-pom modes." The inner segments (represented by thick lines enclosed in dotted representation of the tube) are still to escape from the tube. These inner-segments contribute to relaxation by constraint release and decide the "constraint release pom-pom modes."

as the length of chain with effective Rouse time equals to t. Thus, we can find the stretch relaxation time τ_s of a particular chain segment simply by inverting the function $\tilde{Z}(t)$, to find the time at which $\tilde{Z}(t)$ reaches that segment.

For the constraint release pompom modes, we assign τ_s values that are the same as their orientational relaxation times. Our rationale for this is that constraint release gives a motion of the tube contour similar to that of a simple Rouse chain [Klein (1978); Viovy *et al.* (1991)], which relaxes both stretch and orientation at the same rate [Doi and Edwards (1986)]. The best way of approximating this within the pom-pom model is to set the stretch relaxation time equal to the orientational relaxation time.

C. Flow modification of priority

In Fig. 5, we consider a generic polymer to enquire about the priority one should assign to a particular segment at a particular flow rate (with associated flow timescale τ_F, which is the inverse of the flow rate). Following on from the concepts of "snipped priority" introduced by Read and McLeish (2001), we recognize that at different flow rates, a given segment will have different effective values for its maximum stretch, due to relaxation of other chain segments. The main innovation introduced in Read *et al.* (2011) is to recognize that the critical issue is not [as Read and McLeish (2001) thought] the orientational relaxation time. Instead, we believe it is a question of how chain stretch is transferred from outer chain segments toward the inside of the molecule, which has to do with stretch relaxation times. Segments whose stretch relaxation time is greater than the flow time, $\tau_s > \tau_F$, are able to transfer tension from the outside of the molecule toward the inside, whilst segments with stretch relaxation time less than the flow time, $\tau_s < \tau_F$, cannot themselves stretch and so cannot transfer tension inward, no matter how many chain ends they are attached to.

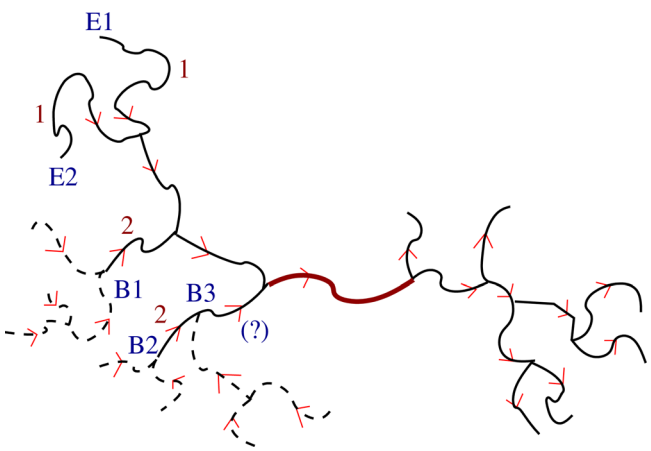

FIG. 5. Assignment of flow-modified priority at flow rate $1/\tau_F$: Segments with $\tau_s < \tau_F$ are described by broken lines. To calculate the effective priority of the thick segment, we travel left along the molecule. At end points like $E1$ and $E2$, where end-segments have $\tau_s > \tau_F$, the segments are assigned a value 1. At a branch point like $B1$, where both the segments have $\tau_s < \tau_F$, the segment before the branch point is assigned a value 2 irrespective of level of branching outward from the branch point. Several possibilities need to be considered in cases where one segment at the branch point has $\tau_s < \tau_F$ and the other has $\tau_s > \tau_F$ (like at branch point B3). If the segment with $\tau_s < \tau_F$ has $\tau_o > \tau_F$, it can maintain a tension difference of 1 and gives a contribution of 1 to the priority sum. Else, we consider the equilibration time of the branch point by calculating the Rouse time of inner segments of B3 including the friction from collapsed side arm. B3 can maintain a tension difference and contributes to the priority sum if this equilibration time is greater than τ_F.

As with the "geometric priority" introduced by Bick and McLeish (1996), we start from a given segment and initially look to one side of it (e.g., the left hand side). Rather than counting chain ends, we examine the relaxation times of each segment as we look outward, as follows. We illustrate some of these cases for a specific molecule in Fig. 5, giving details specific to that molecule in the figure caption.

- For an inner segment with $\tau_s > \tau_F$, if the two outer segments have $\tau_s < \tau_F$, the outer segments cannot stretch. But the current segment can stretch, up to a maximum stretch of 2 (at which point, withdrawal of the branch point will occur). So, we add 2 to the priority sum. Two examples of this are B1 and B2 in Fig. 5.
- If we reach a segment with $\tau_s > \tau_F$ and both the segments outside it have $\tau_s > \tau_F$, all segments can stretch, and we simply proceed to find out what chain structure is beyond the two outer segments.
- For a segment with $\tau_s > \tau_F$, but where only one of the two segments beyond it has $\tau_s > \tau_F$, only one of the subsequent segments can stretch (an example is B3 in Fig. 5). For the subsequent segment that stretches (B2 in the figure), we look to see what is beyond. For the segment that does not stretch (e.g., the dashed side branch at B3), we need to decide whether it provides sufficient friction that this branch point can sustain a significant difference in stretch between the two "stretching" segments. In other words, at the current flow rate, is it possible for the stretch on the inner segment (B3) to be greater than the stretch on the outer segment (B2) by one unit? To answer this, we look at the orientation relaxation time (τ_o) of the side branch.
  - If $\tau_o > \tau_F$, then flow is fast enough to orient the side branch, so the side chain will certainly count toward the priority, and we add one to the priority sum.
  - If, on the other hand, $\tau_o < \tau_F$, more care is required: We calculate an "equilibration time" τ_{eq} for the side branch, as detailed below. If $\tau_{eq} > \tau_F$, then the side branch can support the tension difference, and we add one to the priority sum.

To calculate τ_{eq}, we have implemented a scheme designed specifically for situations in which different side arms along a chain are expected to have greatly varying relaxation times (as is usually the case in, for example, polydisperse industrial resins). The scheme is not expected to work well, for example, in the case of regular polymer combs in which all side arms are of similar length.

We envisage a situation in which all segments outside the side branch have reached their maximum priority, and their branch points are now withdrawn into their tubes. For such a chain configuration, withdrawn branch points count little toward the effective friction for motion of polymer along the tube because chain motion will simply change the degree of withdrawal of the branch point (and so do not require branch point hopping from side arm relaxation). So, we anticipate only a small amount of friction from branch points outside the considered side branch.

Looking inward from the current side branch, we may encounter several shorter side branches with faster orientational relaxation times. We assume these give negligible friction in the current calculation. Eventually, we will typically find a side branch with larger orientational relaxation time than the current one, which will act as a pivot point for local chain motion to equilibrate chain stretch. We measure the length of chain between the current side branch and the first one found inward with larger orientational relaxation time, and this gives an effective spring constant for the local equilibration of stretch due to motion of the side branch. To locally equilibrate the chain stretch, this spring pulls against the friction from the side branch, which can be obtained from its orientation relaxation time (τ_o) using Eq. (1). The ratio of the friction constant to the chain

spring constant, so obtained, gives the equilibration time τ_{eq}, used in the above calculation of priority.

The priority calculation is repeated for the right-hand side of this particular segment, and as with geometric priority, the lower of the two priority sums sets the priority of the segment.

V. ALGORITHMIC IMPLEMENTATION

The linear version of the computational rheology code (previous versions of BoB) already computes the two "fronts" $z(t)$, marking the relaxation of chain ends through tube escape and $\tilde{Z}(t)$, the pivot point about which the retraction is considered at time t. The latter variable defines an approximate Rouse time of a segment of an arbitrarily branched polymer molecule and influences the dynamics of $z(t)$ internally. We identify this Rouse time as the stretch relaxation time of a segment. In the current version of the code, during the relaxation after small step strain, the segments of the polymer molecules store the times at which either $z(t)$ or $\tilde{Z}(t)$ reaches the end of the segment in concern. They, respectively, give the orientational (τ_o) and stretch (τ_s) relaxation times of the segments. The segments also store the friction defined from the time of complete retraction [Eq. (1)]. The prediction of linear viscoelastic moduli already employs the form of sum of a large number of Maxwell modes [Eq. (2)]. They are coarse-grained to have roughly two Maxwell modes in a decade of frequency. With a given choice of Maxwell times (τ_M), the associated weights (g_M) are unique.

To predict the nonlinear flow behavior at a given flow rate, we execute the updated code twice. In the first step, the code generates or reads in the supplied polymer ensemble and executes the algorithm to calculate linear rheology. During this process, it follows time relaxation, and outputs τ_o and τ_s for each of the segments and $\{\tau_M, g_M\}$ associated with the linear relaxation spectrum. In the second pass of the execution, the program uses the same polymer ensemble, now decorated with the relaxation timescales, and hence amenable to computation of flow modified priority variables. During the small strain relaxation in this second execution, the program maintains separate lists accounting for material relaxing through tube escape and through constraint release. For each type of stress relaxation, the lists store the fraction of the relaxation modulus associated with a given priority, subdivided into material with different stretch times (binned in log-scale, typically with 20 bins). The contents of the lists are written to a file when the time reaches the next Maxwell time τ_M, which acts as the orientational relaxation time τ_o for the current modes (for weights at τ_M, we use averages over segments relaxing between the times $\tau_M/1.1$ and $1.1 \times \tau_M$). So, at each Maxwell time, the Maxwell mode is subdivided into a (typically large) number of pom-pom modes with different priority and stretch relaxation time. Once all of the molecules have relaxed, the pompom modes are used to compute the transient stresses in startup shear or startup uniaxial extensional flow.

A. Modeling of HDPE molecules

The HDPE resin (HDB6, The Dow chemical Company) used in this work was synthesized with single-site metallocene catalyst in a continuously stirred tank reactor (CSTR) [Wood-Adams *et al*. (2000)]. The ensemble of molecules in this case can be fully characterized by just two parameters: One characterizing the average molar mass and the other characterizing the average number of branches. Among different possibilities, we choose these two parameters as the weight averaged molar mass (M_W) and the number averaged

branch per molecule (b_m). Because the resin was prepared without any comonomer, the amount of branching is accurately known from NMR. The weight averaged molar mass is known from (Gel permeation chromatography and multi-angle laser light scattering). The M_W and b_m can be recast as the number averaged segment length ($M_{N,S}$) between the branch points and a branching probability (b^U, "up-stream" branching probability). We use a simple scheme introduced in Das *et al.* (2006a) to generate segment-level description of molecules representing the HDPE resin. The algorithm is based on the known statistical distribution of single-site CSTR metallocene resins [Read and McLeish (2001)]. Starting from the end of the molecule at which the last monomer was added, we generate a Flory distributed segment of average length $M_{N,S}$ and use the branching probability to decide if the particular segment would end at a branch point. If it ends at a branch point, we continue adding branches recursively.

B. Modeling of LDPE molecules

We use a Monte Carlo method to generate a statistical representation of LDPE molecules. Tobita (2001) used such a procedure to consider the distribution of polymer structures arising from a free-radical polymerization occurring in a batch reactor (although the basic scheme can be generalized to other reactor types). The basic steps considered are initiation (rate R_i), chain propagation (rate R_p), branching (rate constant k_b), scission (rate constant k_s), chain transfer to small molecules (rate R_f), and termination by combination (rate R_{tc}) or by disproportionation (rate R_{td}). For the batch reaction, this generates a five parameter space of

$\tau = (R_{td} + R_f)/R_p$	Termination
$\beta = R_{tc}/R_p$	Combination
$C_b = k_b/k_p$	Branching
$C_s = k_s/k_p$	Scission
x_f	Final conversion.

For details of the Monte Carlo scheme, and for the relevant equations, we refer the reader to Tobita (2001). Repeated application of the algorithm produces a set of molecules selected on a weight-biased basis. The position and number of all branch points, together with the molecular weight of the strands between them, are known. If sufficient number of branched polymers is generated in this way, then one can interrogate them for statistics of the overall polymer distribution (e.g., molecular weight distribution) or use the generated molecules as input into the BoB algorithm to calculate rheology. The molecules could be used as-generated, but we save computational effort in the rheology calculation by retaining only a fraction of these molecules, chosen uniformly across the range of logarithmic molecular weights generated by the algorithm. This allows us to reduce the number of molecules used in the rheology calculation by a factor of roughly 100; the calculations below used a representative set of around 3000 molecules, but retain many large molecules in the tail of the molecular weight distribution.

We seek to use the above algorithm as a means to model the molecular architectures present in commercial LDPEs, generated in tubular reactors. In the idealized "plug flow" limit, a tubular reactor is equivalent to a batch reactor. However, real reactors are not ideal, and we found it was usually not possible to match experimental molecular weight distributions with a single batch simulation. In the absence of detailed information of

reactor variables and operation, we aimed to produce a reasonable representation of LDPE-like architectures, consistent with experimental data on molecular weight distribution and branching levels (from GPC-MALLS data). Our solution was to consider a superposition of up to three batch processes, with identical reaction parameters τ, β, C_b, and C_s, but different overall conversions x_f. A possible qualitative justification for this is that pure plug flow is unlikely, and different residence times are expected across the cross-section of the reactor tube, leading to different conversions. An alternative suggestion is that broadening of molecular weight distribution is induced by multiple injection points in an idealized tubular reactor.

To reduce the parameter space, we assume no scission, i.e., $C_s = 0$, since its value appeared to be consistently small when left as a free parameter. Although there are several parameters in the reaction scheme, their effects are distinctive. Increasing τ results in shorter chain strands and smaller overall molecular weight. The value of τ could be determined to reasonable accuracy by matching the low-molecular weight tail of the molecular weight distribution. Increasing β increases molecular weight and polydispersity but without greatly affecting branch density or typical molecular weight of linear strands in the molecules. In contrast, increasing C_b increases molecular weight and polydispersity but also increases branching, giving rise to smaller chain strand lengths between branch points.

VI. RESULTS

We have measured rheological responses of six different commercial grade LDPE samples and one HDPE sample to test the computational scheme detailed here. The rheological responses of the LDPE samples are published in a short communication [Read *et al.* (2011)]. Besides the HDPE resin, we select only one of the LDPE resins (LDPE2) here to illustrate the predictions under different assumptions of the modeling. Details of characterization and rheological response measurements can be found in the supplementary online material of our earlier publication [Read *et al.* (2011)]. Molar masses and radius of gyration contractions factor (g-factor) were measured with GPC-MALLS for the LDPE samples. For the HDPE resin, branching was independently measured with NMR. Shear responses were measured on a strain controlled rheometer (ARES, Rheometric scientific) using cone and plate geometry. Optional stretching device (SER, Xpansion instruments) was mounted onto the rheometer to measure the nonlinear elongational flow response.

We use tube dilation exponent $\alpha = 1$ and the branch-point hop-size $p = 1/\sqrt{40}$ that provide a good description of frequency responses of a number of resins with different architectures and chemistry[Das *et al.* (2006a); Das *et al.* (2006b); Chambon *et al.* (2008); Hutchings *et al.* (2012)]. For the HDPE sample, we use $M_e = 1120$ g/mol and $\tau_e = 1.1 \times 10^{-8}$s at 155 °C. The weight average molar mass $M_W = 68\,000$ g/mol and the average number of branches/molecule $b_m = 0.34$ uniquely determine the HDPE resin. These parameters were determined in earlier work [Das *et al.* (2006a)], where the molecular weight and branching parameters were found uniquely from the GPC and NMR measurements, respectively. The rheological parameters provided an excellent fit to the linear rheology of a series of HDB resins.

Presence of comonomer and short-chain branches not accounted in our scheme affect M_e and τ_e [Chen *et al.* (2010)], and we expect them to be quite different for LDPE and HDPE resins. In our data analysis, we heuristically found that $M_e = 1600$ g/mol and $\tau_e = 5.8 \times 10^{-8}$s at 150 °C provide a good description of the small angle oscillatory shear data for six different LDPE resins. By fitting the low-molecular weight tail of the

molar mass distribution, we fix the termination rate parameter $\tau = 1.1 \times 10^{-3}$. We consider the scission rate constant $C_s = 0$. We can fit the full molar mass distribution and the g-factor with different combinations of the other parameters. We found that fits of similar quality to the molar mass distribution and the g-factor naturally gave rise to a distribution of predictions of linear rheology. This is to be expected, since relaxation times of branched molecules depend exponentially on their branching length, so rheology is more sensitive to branching levels than the g-factor. The predicted terminal viscosity, for example, could vary within approximately half a decade. While this was sufficient to rank the LDPE resins in order of terminal viscosity, an imprecise prediction of linear rheology is not a good basis for nonlinear rheology prediction. So, we further constrain the fitting by comparison with the measured linear rheology. We use two sets of such parameters that give equally good fit to the molar mass distribution, the g-factor, and linear rheology. One of the sets (set1) considers the combination rate constant $\beta = 1.2 \times 10^{-4}$ and branching rate constant $C_b = 5 \times 10^{-3}$. The other set (set2) considers $\beta = 1.6 \times 10^{-4}$ and $C_b = 1.8 \times 10^{-2}$. In set1, we use three different final conversions x_f: 74% of the material with $x_f = 0.62$, 13% with $x_f = 0.25$, and the rest with $x_f = 0.05$. In set2, we use two different final conversions with 80% of the resin having $x_f = 0.185$ and the rest having $x_f = 0.032$. We use set1 to compare with experimental data. In the final part of this section, we compare between the predictions of the two sets in the linear and nonlinear flows.

The highly branched nature of LDPE2 is captured by comparing the distribution of the priorities of LDPE2 with that of HDB6 (Fig. 6). The lines in the plot indicate the weight fraction of segments with different geometric priorities. In both resins, the higher priority material accounts for a small fraction (priority one and priority two together account for 98.8% weight for HDB6 and 88.5% weight for LDPE2). For HDB6, the highest priority segment generated is 10. For LDPE2, the maximum priority is 280. We also plot flow modified priorities (symbols). As the flow rate is lowered, the effective priority of the segments changes. At 0.001/s flow rate, the maximum of effective priority for LDPE2 is just 6.

From following the relaxation numerically after a small step strain, we calculate the frequency dependent viscoelastic moduli. Figure 7 shows comparisons of our predictions with experimental data. Similar quantitative predictions are obtained using the same M_e and τ_e for a set of six LDPE [Read *et al.* (2011)] and seven HDPE samples [Das *et al.* (2006a)] having different molar masses, zero-shear viscosities, and melt indices. At the

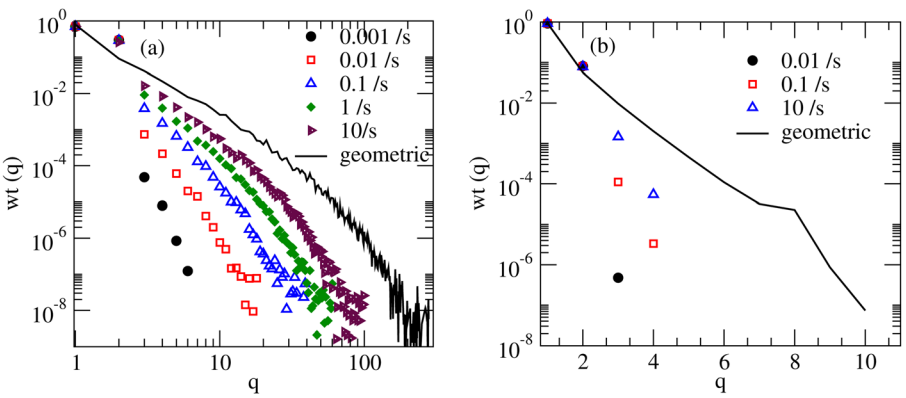

FIG. 6. Geometric (lines) and flow priorities at indicated rates (symbols) for LDPE2 (a) and HDB6 (b) resins.

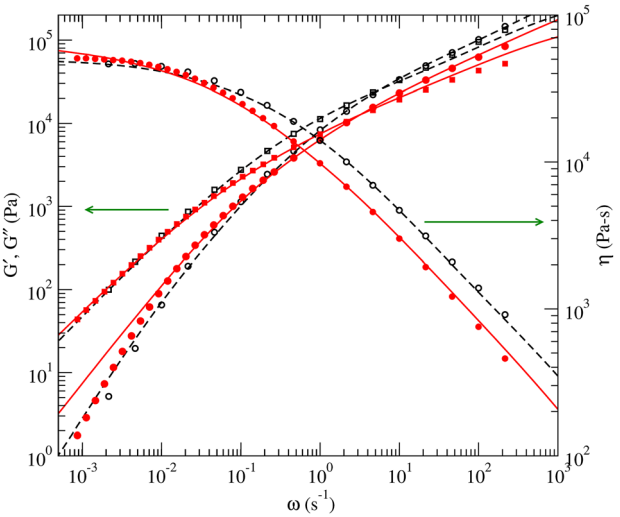

FIG. 7. Viscoelastic moduli and complex viscosity from small angle oscillatory shear experiments (symbols) and predictions (lines) for LDPE2 (filled symbols and solid lines) and HDB6 (open symbols and dashed lines).

lowest frequencies, our prediction for the elastic modulus is higher than the experimental data. The low frequency response is from the stress relaxation in a few highly branched molecules in our calculations. Our modeling assumes that the molecules remain entangled at all stages of relaxation. The discrepancy at low frequencies reflect breakdown of this approximation.

Figure 8 shows the startup stress growth coefficients (transient viscosities) in extension and shear at several rates (symbols) along with predictions from our calculations (solid lines) for LDPE2 and HDB6 resins. We note here that the predictions for LDPE2 are slightly lower than Read *et al*. (2011). In the previous publication, a bug in the code erroneously assigned exactly equal weights to both the constraint release and tube escape modes. The predictions here, and the publicly released version of the code, correct that bug and follow the weight distribution assigned from Eq. (6). The corrected code consistently produces slightly lower predictions than reported in Read *et al*. (2011), with the differences for the LDPE2 resin being typical. For the LDPE2 resin, our calculations represent the linear relaxation with 55 Maxwell modes. At each of these Maxwell modes, separate pom-pom modes account for the distribution in priority and stretch time. For flow rate 0.003/s, we used in total 4587 pom-pom modes to describe the nonlinear flow properties. The typical CPU time for predictions at each flow rate is of order 1 h (on a single node of a Linux machine with Intel Xenon processor).

For LDPE2 resin [Figs. 8(a) and 8(b)], we also show predictions at selected rates where we use geometric priorities (dashed lines) or fully snipped priority (dotted lines) considered in Read and McLeish (2001) to calculate the stress response. The stress response in extensional flow is highly sensitive to the assignment of priority. The geometric priority overpredicts the stress by a large amount, while the fully snipped priority significantly underpredicts the stress. With the LDPE samples containing highly branched structure, the differences in the predictions from the different schemes for assigning the priorities are dramatic. The predictions made using the stretch-based assignment of priority, as detailed in this paper, are superior to either the geometric priority or fully snipped priority predictions (a similar observation can be made for the shear predictions). They also capture well the differences in overall extension hardening behavior between the

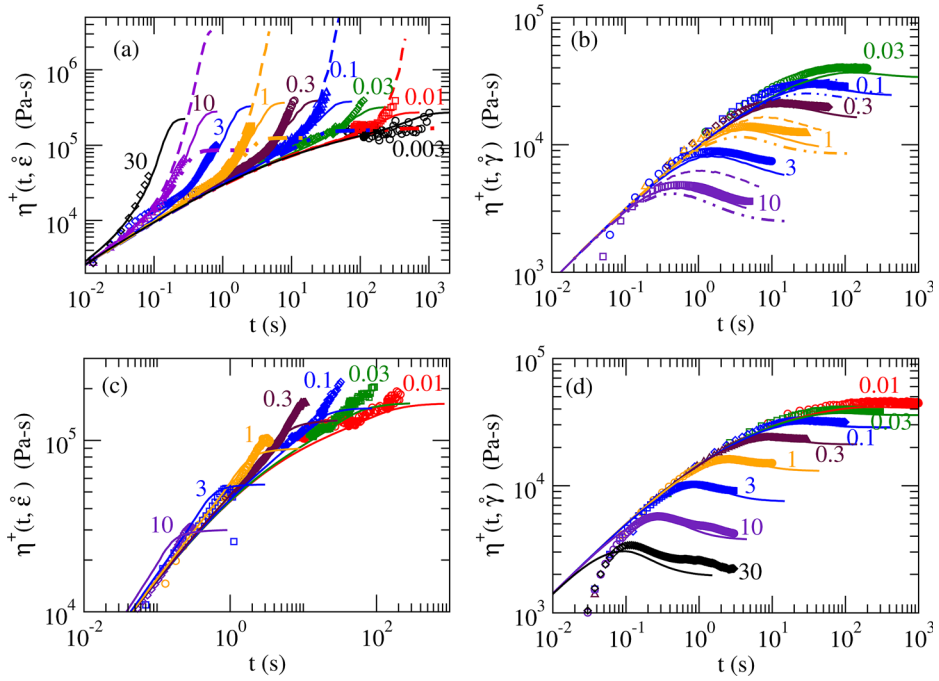

FIG. 8. Startup stress growth coefficients in uniaxial extension [(a) and (c)] and shear [(b) and (d)] at the indicated rates in LDPE2 [(a) and (b)] and HDB6 [(c) and (d)]. The experimental data are plotted as symbols. The solid lines are predictions with flow priorities. For the LDPE2 resin, we also show the predictions using geometric priority (dashed lines) and fully snipped priority (dotted-dashed lines) at rates 0.01, 0.1, 1.0, and 3.0 s^{-1} for uniaxial extension (a) and at rates 0.1, 1.0, and 10.0 s^{-1} for shear (b).

high-density and low-density resins. Nevertheless, it is clear from Figs. 8(a) and 8(c) that the predictions are not perfect, and, in particular, there is a small underprediction of the degree of hardening at the lower extension rates. Discrepancies between our predictions and the data could be due to errors either in our values for stretch relaxation times or in our prediction of flow-dependent priority. Since the geometric priority calculations result in consistent overprediction, we consider it likely that the priority prediction is the likely source of remaining error. Thus, although the stretch-based assignment of priority detailed in this paper (and the approximate algorithm proposed to evaluate internal stretch equilibration times within a molecule) represents an improvement on previous suggested criteria, the scheme remains approximate and open to improvements. We discuss several possible options for this in the concluding section of the paper.

To predict the flow properties of the LDPE resin, we created the molecules by fitting the molar mass distribution and the g-factor. Figure 9(a) shows that similar quality of fit can be obtained by quite different reaction parameters. However, despite the use of different reaction rate parameters to achieve the fit, the frequency dependent viscoelastic moduli are virtually indistinguishable for the two ensembles [Fig. 9(b)]. The startup stress growth coefficients in shear and extension also behave very similarly [Fig. 9(c)]. The distributions of the priorities also are similar [Fig. 9(d)]. This suggests that there is a degree of redundancy in the reaction model parameters: The decrease in conversion x_f in set2 as compared to set1 is largely compensated by the increase in C_b and β. There is also a degree of redundancy in the precise choice of conversions, and their respective weights, for the (up to three) superposed batch processes. Fortunately, as we show here (Fig. 9), different choices of fitting parameters that match GPC-MALLS data and linear rheology

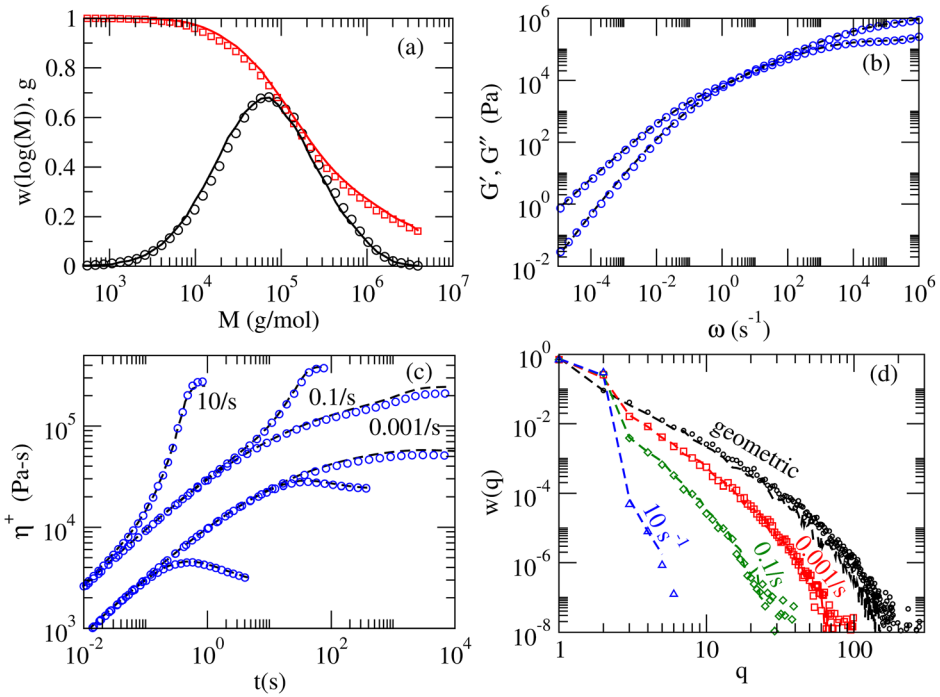

FIG. 9. Predictions for two different set of parameters for modeling LDPE2: (a) Distribution of molar mass and g-factor. Results from set1 are shown as symbols and from set2 are shown as lines. (b) Frequency dependence of the viscous and the elastic moduli for set1 (symbols) and set2 (dashed line) are virtually indistinguishable. (c) Startup stress growth coefficients behave similarly for set1 (symbols) and set2 (dashed lines) in both extension (upper curves) and shear (lower curves) at the indicated flow rates. (d) Priority distributions for set1 (symbols) and set2 (dashed lines) behave similarly at the different flow rates.

give rise to similar predictions for the nonlinear rheology and have similar distributions of molecular architecture.

VII. OUTLOOK

We have described the details of a numerical scheme to compute the nonlinear flow behavior of arbitrarily branched entangled polymer melt by mapping the *in silico* molecular representation of the resin to a set of pom-pom modes. This mapping requires separate modes associated with relaxation by tube escape and constraint release. We generalize the topological concept of priority variables to a flow-dependent priority, which essentially counts the branch points that do not have enough time for relaxation of chain tension, i.e., it is a stretch-based criterion. This depends both on segmental stretch and orientation times and on the timescale of equilibration through coherent oscillation of segments with localized drags.

We validate our scheme by comparing with flow response of two very different commercial resins: A highly branched LDPE and a sparsely branched HDPE resin. The agreement with flow response in both the linear and the nonlinear regimes suggests that one can, in principle, use computational schemes to decide on the synthesis parameters that generate resins with desired flow properties.

The assignment of the priority variables in this work exploits the broad distribution of relaxation times in industrial resins. We use this when considering, at an approximate

level, the internal dynamics of stretch propagation within a randomly branched molecule. This approximation is evident in the calculation of a local stretch equilibration time, τ_{eq}, for a given side branch in Sec. IV C, which exploits a hypothesized wide separation in relaxation times of nearby side branches. As noted above, the scheme is expected to break down for regular comblike molecules and similar well defined structures in which all side arms have similar lengths. Correction of this requires a more detailed consideration of stretch dynamics in such regular molecules. Such work might also lead to improvements to our proposed scheme, and in turn to improvements in predictions for industrial resins, for example, by increasing priority predictions at low flow rates.

An alternative avenue for further investigation concerns the effect of dynamic dilution upon branch-point withdrawal processes and flow-rate dependent priority. Whilst the linear rheology calculation explicitly considers different tube diameters operating at different timescales via the dynamic dilution hypothesis, these considerations are not as explicit in our priority calculation as presented above. In fact, our scheme corresponds to the maximum stretch (priority) being defined in a "flow-tube" whose diameter corresponds to the dilution at the flow time τ_F, the inverse of flow-rate. The reason is that constraint release modes, corresponding to structure on length scales smaller than this flow-tube, relax much faster than the flow time and so are not stretched; only modes corresponding to structure on scales larger than the flow-tube are stretched. However, recent investigations into bimodal blends [Auhl *et al.* (2009); Read *et al.* (2012)] indicate that stretch relaxation dynamics in the presence of constraint release can give rise to complicated and nonintuitive dynamics. The question arises as to whether branch-point withdrawal, leading to maximum stretch, should be considered within the flow tube or perhaps within some smaller tube. Considering a pom-pom like model, Wagner and Rolón-Garrido (2008) assumed branch-point withdrawal should occur in the undiluted tube, giving rise to a larger effective maximum stretch in the diluted tube, and so larger stresses. It is possible that similar physics might be another source of our underprediction of stress at low flow rates. Detailed investigation into this would require a consideration of stretch dynamics in the presence of a broad range of constraint release rates, in particular, focusing on force balance and dynamics in the vicinity of branch points.

Finally, we note that recent experiments on branched polyethylene resins have indicated that there may be stress overshoots prior to the steady state in extensional flow [Wagner and Rolón-Garrido (2008); Alvarez *et al.* (2013); Hoyle *et al.* (2013)], though others dispute these findings [Münstedt and Starý (2013)]. To date, a detailed molecular explanation of the stress overshoots appears to be lacking [for example, the model in Hoyle *et al.* (2013) is phenomenological]. In this work, our focus has been on developing nonlinear rheology predictions based on molecular structure. We have chosen to use the established pom-pom model in our calculations, since this has a molecular basis for each of its parameters. As a result, this present work does not address directly the existence of stress overshoots.

The scheme detailed here is computationally intensive. Thus, we do not envisage the current approach to be used to predict flow properties in a complex flow geometry. Instead, the generated pompom modes can be coarse-grained to a more manageable numbers that predict the same flow property as the original modes but loses the connection to the molecular architecture. Some work along this line has been done for describing large amplitude oscillatory shear experiments [Hoyle (2010)]. These coarse-grained pompom modes in turn can be used to predict the flow properties in more complex geometries [Hassell *et al.* (2008)].

ACKNOWLEDGMENT

The authors thank the Engineering and Physical Sciences Research Council (UK) for funding under the "Microscale Polymer Processing" (μPP) consortium.

References

Alvarez, N. J., J. M. R. Marín, Q. Huang, M. L. Michelsen, and O. Hassager, "Creep measurements confirm steady flow after stress maximum in extension of branched polymer melts," Phys. Rev. Lett. **110**, 168301 (2013).

Auhl, D., P. Chambon, T. C. B. McLeish, and D. J. Read, "Elongational flow of blends of long and short polymers: Effective stretch relaxation time," Phys. Rev. Lett. **103**, 136001 (2009).

Bick, D., and T. C. B. McLeish, "Topological contributions to nonlinear elasticity in branched polymers," Phys. Rev. Lett. **76**, 2587–2590 (1996).

Bisko, G., T. C. B. McLeish, O. G. Harlen, and R. G. Larson, "Theoretical molecular rheology of branched polymers in simple and complex flows: The pom-pom model," Phys. Rev. Lett. **79**, 2352–2355 (1997).

Blackwell, R. J., T. C. B. McLeish, and O. G. Harlen, "Molecular drag-strain coupling in branched polymer melts," J. Rheol. **44**, 121–136 (2000).

Chambon, P., C. M. Fernyhough, K. Im, T. Chang, C. Das, J. Embery, T. C. B. McLeish, and D. J. Read, "Synthesis, temperature gradient interaction chromatography, and rheology of entangled styrene comb polymers," Macromolecules **41**, 5869–5875 (2008).

Chen, X., F. J. Stadler, H. Münstedt, and R. G. Larson, "Method for obtaining tube model parameters for commercial ethene/α-olefin copolymers," J. Rheol. **54**, 393–406 (2010).

Colby, R. H., and M. Rubinstein, "Two-parameter scaling for polymers in θ solvents," Macromolecules **23**, 2753–2757 (1990).

Das, C., D. J. Read, M. A. Kelmanson, and T. C. B. McLeish, "Dynamic scaling in entangled mean-field gelation polymers," Phys. Rev. E **74**, 011404 (2006b).

Das, C., D. J. Read, and T. C. B. McLeish, bob2.5, 2012.

Das, C., N. J. Inkson, D. J. Read, M. A. Kelmanson, and T. C. B. McLeish, "Computational linear rheology of general branch-on-branch polymers," J. Rheol. **50**, 207–235 (2006a).

Doi, M., and S. F. Edwards, *The Theory of Polymer Dynamics* (Clarendon, Oxford, 1986).

de Gennes, P. G., "Reptation of a polymer chain in the presence of fixed obstacles," J. Chem. Phys. **55**, 572–579 (1971).

Hassell, D. G., D. Auhl, T. C. B. McLeish, and M. R. Mackley, "The effect of viscoelasticity on stress fields within polyethylene melt flow for a cross-slot and contraction–expansion slit geometry," Rheol. Acta **47**, 821–834 (2008).

Hoyle, D. M., "Constitutive modelling of branched polymer melts in non-linear response," Ph.D. thesis, University of Leeds, 2010.

Hoyle, D. M., Q. Huang, D. Auhl, D. Hassell, H. K. Rasmussen, A. L. Skov, O. G. Harlen, O. Hassager, and T. C. B. McLeish, "Transient overshoot extensional rheology of long chain branched polyethylenes: Experimental and numerical comparisons between filament stretching and cross-slot flow," J. Rheol. **57**, 293–313 (2013).

Hutchings, L. R., S. M. Kimani, D. M. Hoyle, D. J. Read, C. Das, T. C. B. McLeish, T. Chang, H. Lee, and D. Auhl, "In silico molecular design, synthesis, characterization, and rheology of dendritically branched polymers: Closing the design loop," ACS Macro Lett. **1**, 404–408 (2012).

Inkson, N. J., T. C. B. McLeish, O. G. Harlen, and D. J. Groves, "Predicting low density polyethylene melt rheology in elongational and shear flows with 'pom-pom' constitutive equations," J. Rheol. **43**, 873–896 (1999).

Klein, J., "Evidence for reptation in an entangled polymer," Nature **271**, 143–145 (1978).

Larson, R. G., "Combinatorial rheology of branched polymer melts," Macromolecules **34**, 4556–4571 (2001).

Lee, K., M. R. Mackley, T. C. B. McLeish, T. M. Nicholson, and O. G. Harlen, "Experimental observation and numerical simulation of transient 'stress fangs' within flowing molten polyethylene," J. Rheol. **45**, 1261–1277 (2001).

McLeish, T. C. B., "Hierarchical relaxation in tube models of branched polymers," Europhys. Lett. **6**, 511–516 (1988).

McLeish, T. C. B., and R. G. Larson, "Molecular constitutive equations for a class of branched polymers: The pom-pom polymer," J. Rheol. **42**, 81–110 (1998).

Milner, S. T., and T. C. B. McLeish, "Parameter-free theory for stress relaxation in star polymer melts," Macromolecules **30**, 2159–2166 (1997).

Münstedt, H., and Z. Starý, "Steady states in extensional flow of strain hardening polymer melts and the uncertainties of their determination," J. Rheol. **57**, 1065–1077 (2013).

Park, S. J., S. Shanbhag, and R. G. Larson, "A hierarchical algorithm for predicting the linear viscoelastic properties of polymer melts with long-chain branching," Rheol. Acta **44**, 319–330 (2005).

Read, D. J., and T. C. B. McLeish, "Molecular rheology and statistics of long chain branched metallocene-catalyzed polyolefins," Macromolecules **34**, 1928–1945 (2001).

Read, D. J., D. Auhl, C. Das, J. den Doelder, M. Kapnistos, I. Vittorias, and T. C. B. McLeish, "Linking models of polymerization and dynamics to predict branched polymer structure and flow," Science **333**, 1871–1874 (2011).

Read, D. J., K. Jagannathan, S. K. Sukumaran, and D. Auhl, "A full-chain constitutive model for bidisperse blends of linear polymers," J. Rheol. **56**, 823–873 (2012).

Rubinstein, M., S. Zurek, T. C. B. McLeish, and R. C. Ball, "Relaxation of entangled polymers at the classical gel point," J. Phys. **51**, 757–775 (1990).

Tobita, H., "Simultaneous long-chain branching and random scisson: I. Monte Carlo simulation," J. Polym. Sci., Part B **39**, 391–403 (2001).

van Ruymbeke, E., C. Bailly, R. Keunings, and D. Vlassopoulos, "A general methodology to predict the linear rheology of branched polymers," Macromolecules **39**, 6248–6259 (2006).

Viovy, J. L., M. Rubinstein, and R. H. Colby, "Constraint release in polymer melts: Tube reorganization versus tube dilation," Macromolecules **24**, 3587–3596 (1991).

Wagner, M. H., and V. H. Rolón-Garrido, "Verification of branch point withdrawal in elongational flow of pom-pom polystyrene melt," J. Rheol. **52**, 1049–1068 (2008).

Wang, Z., X. Chen, and R. G. Larson, "Comparing tube models for predicting the linear rheology of branched polymer melts," J. Rheol. **54**, 223–260 (2010).

Wood-Adams, P. M., J. M. Dealy, W. A. deGroot, and D. O. Redwine, "Effect of molecular structure on the linear viscoelastic behavior of polyethylene," Macromolecules **33**, 7489–7499 (2000).